Associative Memory and Segmentation in an Oscillatory Neural Model of the Olfactory Bulb

Ofer Hendin and David Horn

School of Physics and Astronomy
Raymond and Beverly Sackler Faculty of Exact Sciences
Tel-Aviv University, Tel-Aviv 69978, Israel
`hendin@neuron.tau.ac.il` `horn@vm.tau.ac.il`

and

Misha V. Tsodyks

Neurobiology Dept.
Brain Research Building - Weizmann Institute
Rehovot 76100 Israel
`bnmisha@wicc.weizmann.ac.il`

Abstract

We discuss the first few stages of olfactory processing in the framework of a compartmental neural network. Our model consists of inhibitory and excitatory formal neurons with dendrodendritic interactions. We explore the computational properties of this neural network, and point out its possible functional role in the olfactory bulb. We show that in a noisy background the network functions as an associative memory, in spite of the fact that the network operates in an oscillatory mode. When receiving a complex input that is composed of several odors, the network segments it into its components. This is done in two stages. First, multiple odor input is decomposed via a decorrelation mechanism that relies on the temporal independence of odor information originating from spatially distant sources. Secondly, as the recall process of one pattern consists of associative convergence to an oscillatory attractor, multiple inputs are identified by alternate dominance of memory patterns during different sniff cycles. This may give new insight into the rapid sniffing behavior of highly olfactory animals. When one of the odors is much stronger than the rest, the network converges onto it, thus displaying odor masking.

1 INTRODUCTION

Being an outgrowth of the forebrain, the olfactory bulb provides us with an open window to the brain(Davis & Eichenbaum 1991) (Shepherd 1979). It receives all of the chemical sensory input from the olfactory epithelium, and projects a processed transformation of it to the cortex. Although thoroughly explored experimentally, the functionality of the synaptic organization, and the computational properties of the bulb are yet unclear. In this work, we model the bulb using a compartmental approach and combine computational models of neural networks that can be viewed as describing the neural structure and elements of the bulb. By doing that, we establish a description of the whole prospect of the olfactory-bulb circuitry. We propose learning rules that account for the formation of synapses, and adaptive mechanisms that are biologically feasible and enable various computational tasks.

Chemical sensory information enters the bulb via the olfactory nerve that converges onto the glomeruli structures. In the glomeruli, axons of sensory cells terminate on the distal dendrites of excitatory mitral/tufted[1] cells(Shepherd 1992), that in turn project their output to the olfactory cortex and other processing centers. Building on the models of (Hopfield 1991) and (Hendin et al. 1994) we construct a model of the glomerular layer that is capable of performing multiple odor separation from odor signals entering the bulb. This separation is based on temporal independence of the olfactory inputs from different sources. The result is fed into the next layer where comparison with learned memories can take place.

The second computational stage in our model is the *external plexiform layer*. In a recent study (Hendin et al. 1995), we have addressed the form of information processing that takes place in this layer via interactions of projection mitral cells with inhibitory granule cells. These interactions are dendrodendritic in nature, and are mediated by reciprocal synaptic connections. It was shown that the connectivity between cells in this layer may allow for the construction of an associative memory, in spite of the dominance of inhibitory interactions. Here we extend that model into the oscillatory domain, i.e., we show that memory retrieval takes place also under conditions that resemble the oscillations observed experimentally(Laurent & Davidowitz 1994).

We combine the various processing stages while following the layered architecture of the bulb. The gross features of experimentally observed electrical activity are obtained. We show how the neuronal circuitry in the bulb may give rise to sub-threshold oscillations in membrane potential of projection neurons, while maintaining associative memory as well. We also show how these oscillations enable pattern segmentation(Malsburg & Schneider 1986) (Malsburg & Buhmann 1992), thus we indicate a possible role for their existence.

In the next section we describe the models that are used at each computation stage. Section 3 is concerned with the construction of a comprehensive neural network based on these models using a compartmental approach. We discuss oscillations and segmentation in section 4, and present numerical results that support our theory.

[1] Henceforth we shall refer to mitral cells only, since mitral and tufted cells are similar in their behavior and function.

2 Autonomous Models of the Bulb Layers

2.1 Glomerular Layer

The first synapse of the olfactory sensory neurons is in the glomeruli structures. There, sensory axons terminate on the distal dendrites of mitral/tufted cells. The latter are taken to represent odor space. Following (Hopfield 1991) we assume that the mitral cells, whose membrane potential will be denoted by u_j, undergo the dynamics

$$\frac{du_j}{dt} = -\frac{u_j}{\tau} - \sum_k T_{jk} u_k + I_j(t). \tag{1}$$

T_{jk} describes an effective dendro-dendritic interaction between excitatory mitral cells induced by inhibitory periglomerular cells, with a specific structure to which we will return later. I_j represents the synaptic input that reaches cell number j. This input is composed of signals from $q = 1, \cdots, K$ different sources that are assumed to have independent temporal fluctuations $a_q(t)$:

$$I_j(t) = \sum_{q=1}^{K} S_j^q a_q(t) \tag{2}$$

The parameters S_j^q represent the composition of odorant number q in a vector space spanned by the mitral cells. Given an appropriate learning rule for the coupling matrix T, (Hopfield 1991) has shown that this network can perform the task of "*blind separation*" of odors by rapid adaptation. Assuming that the lateral connections between neigbhoring glomeruli are weak, we shall consider each glomerulus as an independent unit. This implies that the matrix T has block-diagonal structure, i.e. it connects only mitral cells that belong to the same glomeruli. Mathematically this is equivalent to the "model of horizontal replicas" in (Hendin et al. 1994). The result is that within each group of cells belonging to a glomerulus, only K neurons remain active. They correspond to the leading components in all K odors of the input that reaches this glomerulus. Over the whole layer we will then find a single (winning) neuron per each fluctuating odor for each glomerulus.

In the compartmental approach that will be developed below, u_i represents membrane potential in the distal part of the dendritic tree. The leading dendritic potentials feed into the following stages of computation.

2.2 External Plexiform Layer - EPL

The second processing stage is related to a section of mitral cell dendrites that are located in the proximity of the soma, and interact with inhibitory granule cells. Following our mathematical formulation in (Hendin et al. 1995), we denote the membrane potential of mitral dendrites at the external plexiform layer by continuous variables m, and that of a granule cell by g. Their dendrodendritic interactions will be denoted by matrices:

J - granule synapse on mitral cells,

W - mitral synapse on granule cells,

K - granule synapse on granule cells,

excluding any excitatory-excitatory couplings. In order to induce oscillations, we incorporate into the granule cells a special class g^n that has local interactions with mitral cells, as well as local excitatory feedback currents $j_i = \alpha m_i$ to the mitral cell. The resulting set of equations is:

$$M_i = \sigma(m_i) \quad \text{with} \quad \frac{dm_i}{dt} = -\frac{m_i}{\tau_m} - \sum_j J_{ij} G_j - \lambda_{gm} G_i^n + I_i + j_i \tag{3}$$

$$G_i = \sigma(g_i) \quad \text{with} \quad \frac{dg_i}{dt} = -\frac{g_i}{\tau_g} + \sum_j W_{ij} M_j - \sum_j K_{ij} G_j$$

$$G_i^n = \sigma(g_i^n) \quad \text{with} \quad \frac{dg_i^n}{dt} = -\frac{g_i^n}{\tau_g} + \lambda_{mg} M_i$$

The variables M (G,G^n) denote the rates of neurotransmitter release from a mitral (granule) cell with membrane potential m (g,g^n). We assume that these rates are sigmoid functions of the membrane potentials, thus introducing the nonlinearity that is essential for the associative memory that we construct. For simplicity, we choose in the present work to use the *limited linear threshold* approximation of the sigmoid function:

$$\sigma(x) \approx \mathcal{L}(x) = \begin{cases} \beta\tilde{x} & x \geq \tilde{x} \\ \beta x & 0 < x \leq \tilde{x} \\ 0 & x \leq 0 \end{cases} \tag{4}$$

Memory patterns will be defined on the mitral cells, since they are the ones that project to higher layers of the cortex. With the learning rules that will be described later, this network performs retrieval of learned activity patterns when presented with a partial input I_i.

The models which describe the Glomerular layer and EPL relate to different parts of dendritic trees that belong to one type of neurons, the excitatory mitral cells. We next introduce a comprehensive model network whose cells are described as compartmental compositions of dendritic elements.

3 Compartmental Model of Mitral Cells

The layered structure of the olfactory bulb (shown schematically in figure 1) is traversed by the dendrites of projection mitral cells. This fact makes them good candidates for piecewise modeling of the different layers in terms of functional units. Making practical use of this architecture, we divide each mitral cell into three compartments. A *distal* compartment that stands for the dendritic tree that resides in the glomerular layer, the *proximal* compartment describing the inner part of the dendritic tree that passes through the *external plexiform layer* and reaches the soma, and a third compartment that describes mitral cell bodies and their axonal outputs (figure 2).

Each of the compartments is used as a building block for a local network responsible for a processing task. The compartments are then joined to give a full description of the individual neuron. The result is a network of complex neurons with well defined roles for the different compartments.

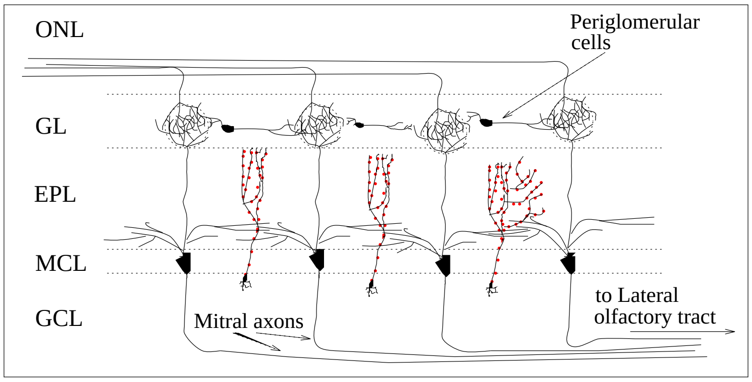

Figure 1: Illustration of the *Olfactory Bulb* layered architecture.
ONL - Olfactory Nerve Layer, GL - Glomeruli Layer, EPL - External Plexiform Layer, MCL - Mitral Cell Layer, GCL - Granule Cell Layer.

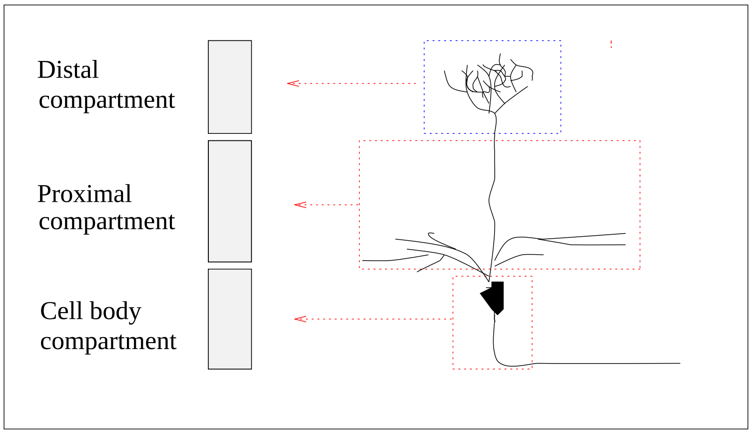

Figure 2: Schematic diagram of a compartmental division of a mitral cell.

3.1 Definitions

We redefine the various variables to be used in the compartmental model.
Distal Compartment This has a similar structure to the one defined by equations 1 and 2 using the notation:

- u_i - membrane potential of the i'th distal compartment.
- I_i - synaptic input from the olfactory nerve to the i'th distal compartment.
- T_{ij} -effective synaptic conductance between the j'th and the i'th compartments of mitral cells of the same glomerulus.

Proximal Compartment
Here we will rely on equations (3) where dendrites of mitral cells interact with those of granular cells. Keeping our notation, we set:

- m_i - membrane potential of the i'th proximal compartment.
- g_j - membrane potential of the j'th granule cell.
- g_i^n - membrane potential of the i'th granule cell that is nearest to mitral cell m_i.
- J_{ij},W_{ij},K_{ij} - synaptic conductance between cells in the EPL.
- j_i - feedback current to a mitral cell.

Note that the number of granule cells is much larger than that of the mitral cells in the OB and in our model. We have pointed out (Hendin et al. 1995) the significance of this difference and its importance in facilitating a larger memory capacity (see also (Frolov & Muraviev 1988)).

Cell Body Compartment

At the cell body, we assume that leaky integration of the dendritic potential takes place. This integration process stops when the threshold for spike generation is crossed. An *"integrate and fire"* function describes this process.

The argument s stands for the membrane potential at the soma, that integrates the currents derived from the dendrites of the cell:

$$s_i = \int_{t_s}^{t} \left(-\frac{s_i}{\tau_s} + \lambda_{sm} \frac{m_i}{\tau_s} \right) dt' \tag{5}$$

After a spike is released, the soma potential is reset to zero and following that, the integration process resumes. t_s denotes the time of the latest spike release. We neglect refractory periods in the present discussion.

3.2 Complete Cells and Network

Let us now construct the neural network of the olfactory bulb using a compartmental description of the functional layers (see Appendix). u_i is identified with the membrane potential of the first compartment, m_i with the second, and s_i with the third. We shall neglect any leakage current other than the capacitor. The incoming currents will be replaced by synaptic currents in all compartments, while in the first compartment we include also external sensory inputs. The resulting set of equations is the following:

$$\frac{du_i}{dt} = -\frac{u_i}{\tau_m} - \sum_j T_{ij} u_j + \lambda_{um} \frac{m_i}{\tau_m} + I_i(t) \tag{6}$$

$$\frac{dm_i}{dt} = -\frac{2m_i}{\tau_m} - \sum_j J_{ij} G_j - \lambda_{mg} G_i^n + \lambda_{mu} \frac{u_i}{\tau_m} + \lambda_{ms} \frac{s_i}{\tau_m} + j_i \tag{7}$$

$$\frac{dg_i}{dt} = -\frac{g_i}{\tau_g} + \sum_j W_{ij} M_j - \sum_j K_{ij} G_j \tag{8}$$

$$\frac{dg_i^n}{dt} = -\frac{g_i^n}{\tau_g} + \lambda_{mg} M_i \tag{9}$$

$$\frac{ds_i}{dt} = -\frac{s_i}{\tau_s} + \lambda_{sm}\frac{m_i}{\tau_s} \tag{10}$$

The constants λ denote conductivity (coupling) of different currents to the compartments. The nonlinearity of these equations is weak, and is brought about by setting lower and upper limits (that are not necessarily reached) on the values of the membrane potential at the different compartments[2]. The last equation is valid only when the potential of the soma s_i is below its firing threshold. After firing s_i is reset to 0.

The input to this system is given by the external currents I_i in equation (6). The output is composed of spike trains of the mitral cells projected through their axons to the cortex. These spikes, generated whenever s_i reach their thresholds, are not represented explicitely in the above set of equations.

3.3 Adaptive Behavior and Learning

Learning follows different rules in the first two compartments. In the glomeruli, where the first compartment resides, learning is assumed to be rather rapid and to occur whenever a new input is presented. This is much like an adaptation process, and it is governed by the following learning rule (Hopfield 1991):

$$\delta T_{ij} = \bar{u_i}\bar{u_j}[\delta + \epsilon(\bar{u_i} - \gamma\bar{u_j})] \tag{11}$$

The bar notation refers to high-pass filtering of the potentials. The matrix element T_{ij} changes with time according to equation 11 but is not allowed to turn negative. This form of synaptic modification gives rise to a temporary weight adjustment rather than a prolonged change of the weights. In our model this rule is supposed to be valid for the efective interaction between mitral cells that belong to a single glomerulus.

In the proximal compartment, we assume that learning takes place during training periods (see, e.g., (Hasselmo 1993), (Hasselmo & Bower 1993)) when the connection matrices of the proximal compartment change according to the following Hebb and anti-Hebb learning rules:

$$\begin{aligned}
\delta J_{ij} &= \frac{\epsilon}{N}(1 - M_i)G_j \qquad (12)\\
\delta W_{ij} &= \frac{\rho}{N}G_i M_j \\
\delta K_{ij} &= \frac{\kappa}{N_g}[(1 - G_i)G_j + G_i(1 - G_j)]
\end{aligned}$$

The constants ϵ, ρ, and κ, define the learning rates. Learning takes place by presenting u_i inputs to the EPL network after it has been initialized with random connectivity. With each new pattern presented, the membrane potentials of the cells are set to small random values, in order to remove the trace of the last pattern of activity. They are then allowed

[2]Due to the "realistic" aspiration of this description, we may not disregard the fact that membrane potential of neurons can normally assumes arbitrary value, but is rather bounded. We mark these bounds with V_{min}, V_{max} and shall refer to the specific values when discussing simulations.

to evolve to their asymptotic activity. The resulting M and G values are then used for updating the connectivity matrices.[3]

No learning is assumed between mitral cells and their associated local granule cells (g^n). This interaction is assumed to regulate the subthreshold oscillatory behavior of the network (discussed later) that is known to be almost independent of the stimulus strength.

4 Oscillations and Segmentation

4.1 Oscillations in the EPL Network

We have previously shown, (Hendin et al. 1995), that the EPL model network without the local granular cells g^n is an associative memory that converges to a stationary attractor (fixed point). This was done using the Heavyside step function as an approximation to the nonlinear relation $M_i = \sigma(m_i)$. In the present paper, we use the limited linear threshold approximation that may be closer to reality. As a result, M_i are continuous variables, and the network possesses oscillatory transients while converging to its final steady state attractor. The dissipative character of the interactions still leads to a stationary state.

In order to avoid dissipation into fixed points and replace it by oscillatory behavior, one has to incorporate into the network local excitatory feedback currents and local interactions with granule cells. Then we can reach a regime where constant input gives rise to sustained oscillations that last for the duration of the input. Once the input is turned off, the oscillations die out, and the activity returns to random (background) activity. It is important to note that the frequency of oscillations is chiefly determined by the constants λ_{gm} and λ_{mg}, however, the coupling to granule cells that is mediated via J_{ij} has an effect of broadening the spectral curve of the oscillatory response.

4.2 Simulation results

We have simulated a network composed of 300 mitral cells m_i, 300 local granule cells g_i^n and 300 other granule cells g_j. In general it is preferrable to allow for much more granule cells in order to improve the capacity of the network. In the present section we wish to demonstrate oscillations and segmentation into two patterns, therefore a restricted structure of granule cells will work as well. We refer to (Hendin et al. 1995) for a discussion of the capacity.

The 300 mitral cells are divided among 12 glomeruli, each containing 25 of them that interact with one another in the distal compartment. The result of this interaction leads to approximately one active u_i per glomerulus for each odor. Starting with the single odor problem we show in figures (3) and (4) results for the EPL network in which the memory patterns are composed of a fraction of $f = 0.025$ active mitral cells(Stewart et al. 1977) (Sharp et al. 1977). As input we have used constant u_i that formed a distorted version of one of the stored patterns, in which 2 bits were randomly flipped. The dynamics of the network was simulated during one second, in which the response to a stationary input that lasted for 350ms was observed. The differential equations that govern the dynamics were integrated using the Runge-Kutta method. A list of the parameters that were used is given in Table 1 below.

[3] This algorithm was proposed in (Hendin et al. 1995) within the nonoscillatory mode, with inactive g^n neurons. We have verified that it works also in the oscillatory network described here.

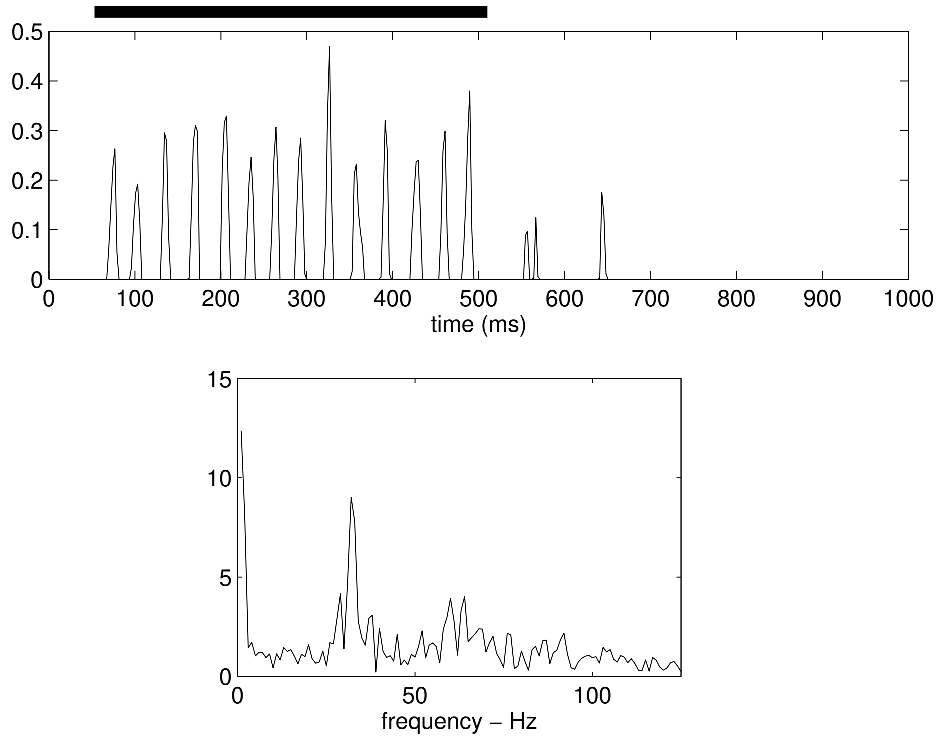

Figure 3: Membrane potential of one of the active neurons (top), and its power spectrum (bottom). The bar on top represents the duration of the signal.

Figure (3) shows the membrane potential of one of the active neurons, and its power spectrum. We see that the oscillatory response to the constant input is dominated by a frequency of about 35Hz. The relatively broad power spectrum is due to the effect of long range interactions (J_{ij}).

The activity of the whole EPL network is presented in Fig. (4). The lower box shows the input, that contained two superfluous bits removed by the associative recall process. The upper box shows rapid convergence into the correct pattern. Each pixel represents an activity peak of a single neuron, as shown above in Fig. (3). The synchronous rhythmic activity of relatively high amplitudes continues for the duration of the input. Neurons that are not part of the memory are either quiescent or are randomly active, but never in phase with the pattern. That is, the convergence and recall properties of the network are maintained even though the membrane potentials of single neurons undergo oscillations. Once the input is turned off, the amplitude decreases and spontaneous background activity resumes.

4.3 Segmentation

When the input is composed of a few odorants, each of which is known to the system, we expect the neural response to indicate that we face few different odors. In the first compartment of our model we perform blind separation of these odors, a process that is based on the assumption that the different sources have temporal variations that are independent

τ_m	=	$20ms$	λ_{mg}	=	0.53	ϵ	=	5
τ_g	=	$10ms$	λ_{um}	=	0.2	ρ	=	1
τ_s	=	$20ms$	λ_{ms}	=	0.1	κ	=	1
α	=	0.25	λ_{mu}	=	0.2	v_{min}	=	-0.25

Table 1. Values of the various parameters that were used in the simulation

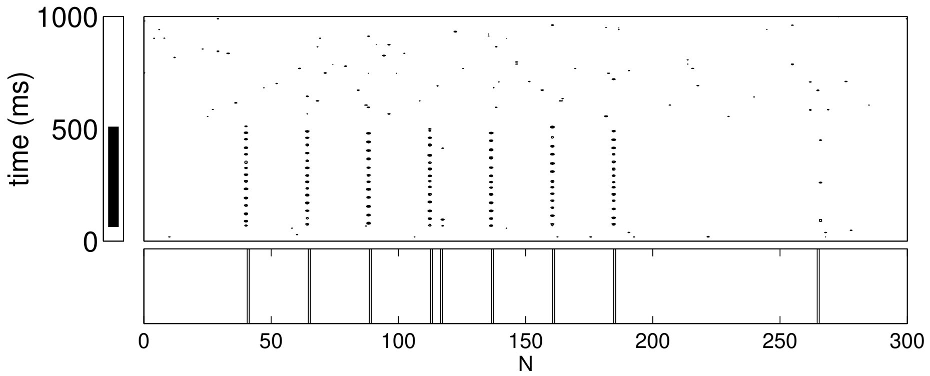

Figure 4: One second of simulated activity in the external plexiform layer evoked in response to a short stimulus (from $t = 150ms$ to $t = 500ms$) that is constant in time.
Top box: Activity of mitral membrane potential. Dark pixels represent values of $m_i > 0$. The x-axis represents the index $i = 1, \cdots 300$ of the neuron, and the y-axis is time. The duration of the input pattern is denoted by the bar in the left box.
Lower box: Input pattern defined on the 300 mitral cells.

of one another. This leaves at most one active input for each odor in each glomerulus. When fed to the second compartment, the EPL model, we have a competition between these inputs, since each odor corresponds to a different memory of this neural network. The question is, then, how does the EPL cope with this situation.

In our oscillatory model of associative memory, spurious states do not exist. By that we mean that only one cell assembly can be coherently active while performing error correction and pattern completion. It is true, however, that a complex input that is composed of more than one pattern, may still lead to higher than spontaneous activity in some of the neurons, that will typically be out of phase and of lower frequency and amplitude than the dominant memory pattern . In other words, this process is a winner-take-all mechanism in which only one memory pattern can be coherently active at a time.

This leads then naturally to the interpretation that in every inhalation period only one pattern is perceived. It suffices for its input to be stronger for a brief interval of few milliseconds in order that this pattern will survive as the only coherently active memory in the EPL. The exhalation provides for a reset [4] of the neural system, that makes it perfectly

[4] It is known (Lazard et. al. 1991) that odorant molecules stimulating the olfactory epithelium are rapidly removed by intrinsic mechanisms. It follows that during the exhalation phase of the breathing cycle, the olfactory nerve is almost not inervated. We regard this period as a recovery time for the internal activity, in which the system may return to spontaneous activity.

possible for another odor to be the dominant component in the next inhalation. Thus one can obtain random alternation between convergence to each of the memories, leading to perfect temporal segmentation of the input.

4.4 Simulation results

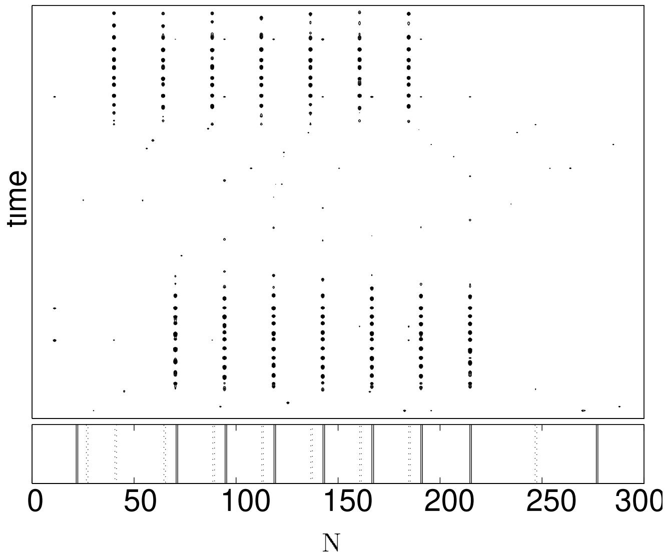

Figure 5: Activity in the EPL network while it is exposed to an input pattern composed of two memories. The input is represented in the lower box by dash or solid lines that denote members of one odor pattern or another. The time scale is 1 sec and includes two inhalation periods in which both odors are presented with the same intensity, yet in each cycle only one of the odors is retrieved.

In this Section we demonstrate how our network performs odor segmentation. For the sake of simplicity, we model the olfactory bulb of an animal that completes two breathing cycles within one second. During this period, we simulate the activity of the network in response to an input that is composed of two memorized odor patterns. The sniff cycle is simulated as a simple modulation of the input by the positive phase of a sine wave, while the negative phase is considered to transfer zero input.

Shown in Fig. 5 are the two input patterns and the resulting excitatory activity in the EPL. Clearly, the activity in the network converged quickly to one of the stored patterns. As the input was turned off (by the simulated process of exhalation), the activity decayed back to background level. On the following inhalation, the activity converged to the second odorant in the input which happend to be slightly stronger this time. Traces of the activity in the previously active cell assembly are still present, but this time they are out of phase, and of lower amplitude.

Figure 6 displays the overlap of membrane potentials of excitatory mitral cells in the EPL with each of the stored patterns. This is the same simulation represented in Fig. 5. One can see that in each inhalation cycle, the activity overlap of one memory pattern dominates.

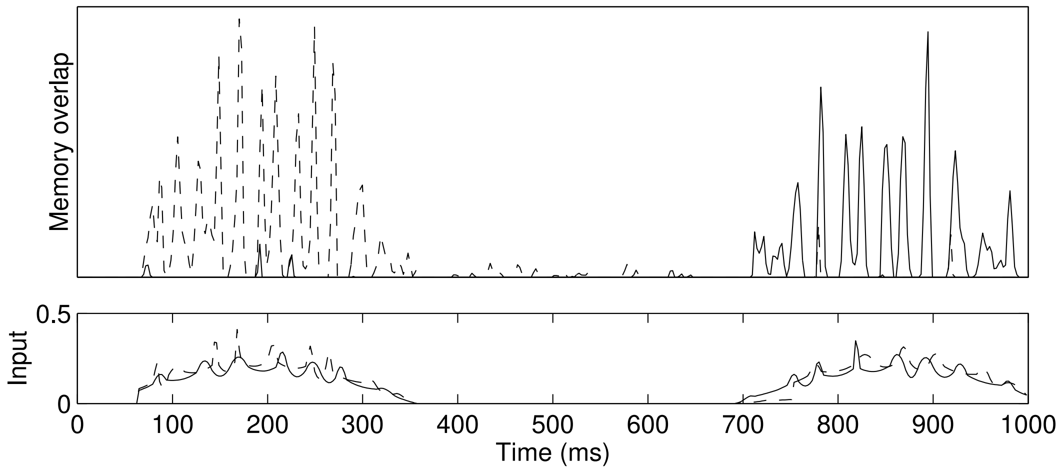

Figure 6: The overlap of two odor memories with the activity of the network responding to a mixed and distorted version of these two odors. The activity converges to one memory pattern in the first inhalation. After relaxation (during exhalation) the other memory dominates. This is an alternative representation to the simulation in Fig.5

Clearly, we chose a situation in which two successive inhalations are characterized by the dominance of different patterns. This is not always the case. However, the uncorrelated temporal structure of the two sources guarantees that the probability of activation of each of the memories corresponds to its relative abundance in the mixed input.

To demonstrate the coherence between neurons that belong to the same cell assembly, we compare in Fig. 7 the normalized correlation coefficients of two neurons that belong either to the same cell assembly or to two different cell assemblies. A large positive component shows that neurons in the same memory are in phase, while correlations of neurons from different memories have negative coefficients, indicating that the neurons oscillate out of phase.

5 Conclusions

We have developed a compartmental model of the olfactory bulb. Although only gross features are considered, our simulated neural behavior is in good agreement with the characteristics of experimental results. We view the olfactory bulb as an early stage processor, and the olfactory input as a flow of particularly noisy chemico-temporal information. We show that the circuitry of the olfactory bulb may play a substantial role in the recognition of odor input.

We regard the layered architecture of the bulb as composed of different processing stages. Each stage performs one computational task, and the combination yields results that are biologically plausible.

The first processing stage of our model consists of an adaptive network that performs blind separation of odors (Hendin et al. 1994) and is assumed to be located at the glomerui. This helps to sharpen the input to the next computation layers. The active mitral cells are the ones reacting to odor molecules that are of highest concentration in the stimulus. This

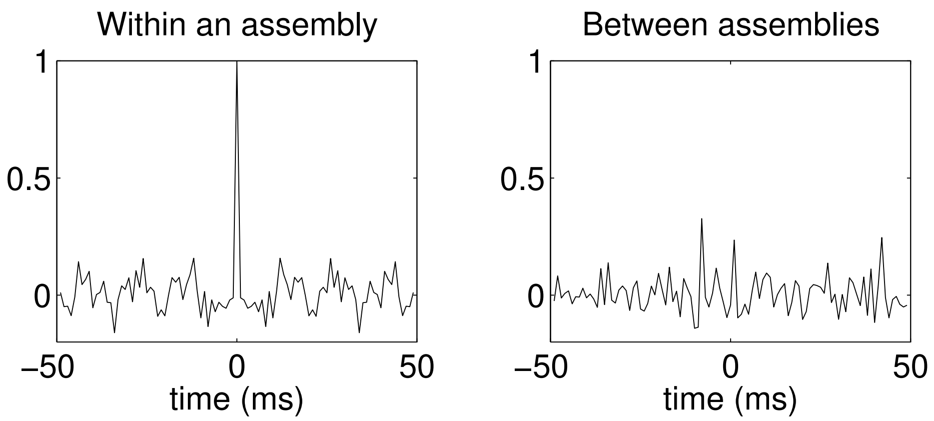

Figure 7: The normalized correlation coefficients between two neurons that belong to the same cell assembly (left box), and to different assemblies (right box).

computational stage is convenient but not really crucial for the rest of the analysis. If the input is naturally sparse, the rest of the network could perform its tasks without this first filter.

The second computing stage of the model, the external plexiform layer, possesses a dendritic network that is capable of learning through synaptic modification. When performing a memory recall task, an incoming pattern activates neurons within the basin of attraction of a known memory. The associative recall mechanism drives the dendritic potential of mitral cells to match a known activity pattern, while correcting errors in the input.

The last stage of the model network is that of the cell body. We model the soma by a leaky integrator. Characteristically, when a given firing threshold is crossed, the soma potential is reset to zero. The spiking output of the soma reflects all of the computational processing that takes place in the dendrites, thus it serves as the correct axonal description of the cortical input from the olfactory bulb.

As a whole, the model presented here shows that the neural network constituting the olfactory bulb is capable of performing odor discrimination on the basis of temporal independence, odor recognition by associative memory principles, and segmentation of complex odor stimuli. This is implemented using non-linear dendrodendritic interactions between neurons.

Odor discrimination is an important processing task in olfaction. According to our scheme, each sniff samples the odor stimulus in a slightly different fashion. In the bulb, the dendritic output from the glomeruli carries the information of the different odorants in terms of elevated membrane potentials of the mitral cells. A relatively short, coherent, temporal dominance in the activity of a group of mitral cells that are part of a memorized odor pattern, leads to convergence onto a memory attractor. Once a memory cell assembly is active, all of the other cells in the network are either quiescent or weakly active and out of phase relative to the recalled memory. In other words, the oscillatory activity coincides with only one of the input stimuli.

Our model predicts that if a molecular combination of one odorant in a complex odor input dominates all the others, then the neural response will match that of the strong odor and will not reflect in any significant fashion the existence of the weak odorants. This result corresponds to the phenomenon of odor masking.

If different odorants in the input are of comparable intensities, the activity of the mitral cells will correspond at different inhalation periods to different odorants. Due to randomness in the temporal dominance of an odorant in the input, each sniff may lead to memory recall of a different component of the input. This may explain the elevated sniff rates that are observed in animals when they encounter odors in their environment.

In our simulations we have used similar numbers of mitral and granule cells. We have already shown (Hendin et al. 1995) that using larger ratios of granule/mitral populations may improve the capacity of the associative memory. Here this larger number of granule cells was not needed, because all we wanted to demonstrate was that memory learning and recall can take place in the oscillatory network, and that segmentation of two odors can be achieved. This may also be generalized to represent segmentation of more odorants, similarly to how blind separation of more than two odors may be computed in the glomeruli (Hendin et al. 1994).

We conclude that, although our network uses only schematic descriptions of the neural elements and dendritic currents in the olfactory bulb, it may account for cognitive abilities and behavioral patterns. Its activity resembles electrophysiological results (Skarda & Freeman 1987), (Laurent & Davidowitz 1994), displaying oscillations and formation of cell assemblies that are odor specific. We hope that future experimental studies will substantiate the associative memory aspect of the olfactory bulb and demonstrate how it uses its oscillatory activity to achieve odor segmentation.

Appendix

A. Basics of Compartmental Models

The total current i_{m_j} **leaking out** of the membrane of the j'th compartment is the difference of the incoming and outgoing axial currents:

$$i_{m_j} = i_{j-1,j} - i_{j+1,j} \tag{13}$$

This current also equals:

$$i_{m_j} = I_{ion_j} + C_{m_j} \frac{dV_j}{dt} \tag{14}$$

Every additional current in the radial direction must be added to the right side of this equation. The longitude current is expressed as the gradient of the potential between two successive compartments divided by the axial resistance of the two:

$$i_{j-1,j} = \frac{V_{j-1} - V_j}{r_{j-1,j}} \tag{15}$$

So, we can express i_{m_j} as a function of the membrane potential:

$$i_{m_j} = \frac{V_{j-1} - V_j}{r_{j-1,j}} - \frac{V_j - V_{j+1}}{r_{j,j+1}} \tag{16}$$

For the first and last compartment in a chain only one term is present in the right hand side.

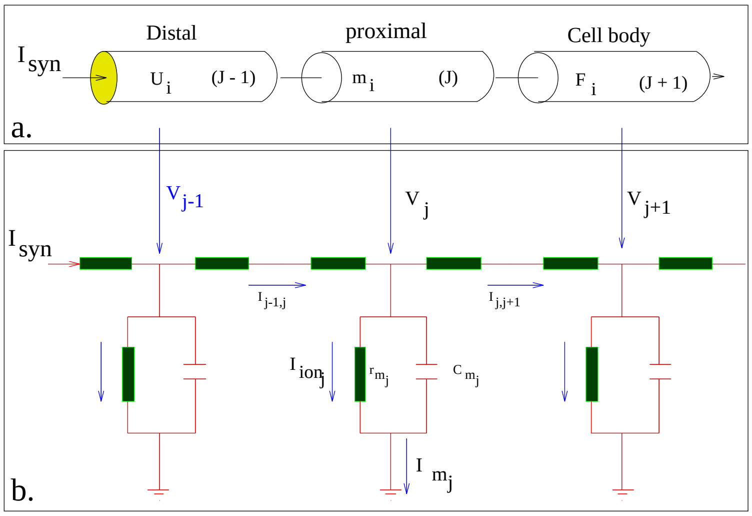

Figure 8: Equivalent circuit for the compartmental model of a mitral cell. It is composed of a chain of two successive small cylinder segments (passive dendritic membrane), plus one compartment to symbol the cell body (active membrane).

References

(Davis & Eichenbaum 1991) Davis J. L. and Eichenbaum H. (eds): Olfaction. MIT press (1991).

(Frolov & Muraviev 1988) Frolov A. and Muraviev I.: Informational characteristics of neural networks. Moscow, Nauka. (In Russian) (1988).

(Hasselmo 1993) Michael E. Hasselmo: Acetylcholin and Learning in a Cortical Associative Memory. Neural Computation Vol. 5, No. 1 (1993).

(Hasselmo & Bower 1993) Hasselmo M.E. and Bower J.M.: Acetylcholine and memory. Trends in Neurosciences, 16(6) pp. 218-22 (1993).

(Hendin et al. 1994) Hendin O. Horn D. and Hopfield J. J.: Decomposition of a Mixture of Signals in a Model of the Olfactory Bulb. Proc. Natl. Acad. Sci. Vol. 91 No. 13 pp. 5942-5946 (1994).

(Hendin et al. 1995) Hendin O. Horn D. and Tsodyks M. V.: The Role of Inhibition in an Associative Memory Model of the Olfactory Bulb. Accepted for publication in the Journal of computational neuroscience (1995).

(Hopfield 1991) Hopfield J. J.: Olfactory computation and object perception. Proc. Natl. Acad. Sci. USA, pp. 6462-6466 (1991).

(Laurent & Davidowitz 1994) Laurent G. and Davidowitz H.: Encoding of olfactory information with oscillating neural assemblies. Science, vol. 265, pp. 1872-1875 (1994).

(Lazard et. al. 1991) D.Lazard, K. Zupko, Y. Poria, P. Nef, J.Lazarovits, S. Horn, M. Khen, and D. Lancet: Odorant signal termination by olfactory UDP glucuronosyl transferase. Nature. Vol. 349 28 Feb. pp. 790-793 (1991).

(Malsburg & Schneider 1986) C. von der Malsburg and W. Schneider,: Biol. Cyber. 54, pp. 29-40 (1986).

(Malsburg & Buhmann 1992) C. von der Malsburg and J. Buhmann, Biol. Cyber. 67, pp. 233-242 (1992).

(Shepherd 1979) Shepherd G. M.: The Synaptic Organization of the Brain, Oxford Univ. Press, New York (1979).

(Shepherd 1992) Shepherd G. M.: Modules for molecules. Nature 358, pp. 457-458 (1992).

(Stewart et al. 1977) Stewart, W. B. Kauer J. S. and Shepherd G. M.: Functional organization in rat olfactory bulb analyzed by the 2-deoxyglucose method. J Comp. Neurol. 185, pp. 715-734 (1979).

(Sharp et al. 1977) Sharp, F. R. Kauer J. S. and Shepherd G. M.: Local sites of activity related glucose metabolism in rat olfactory bulb during olfactory stimulation. Brain Res. 98. pp.596-600 (1975).

(Skarda & Freeman 1987) Skarda C. A. and Freeman W. J.: How brains make chaos in order to make sense of the world. Behavioral and Brain Sci. 10, pp. 161-195 (1987).